

***IN SITU* MONITORING OF LASER MODIFICATION PROCESS IN HUMAN CATARACTOUS LENS AND PORCINE CORNEA USING COHERENCE TOMOGRAPHY**

**V. Kamensky, F. Feldchtein, V. Gelikonov, L. Snopova, S. Muraviov, A. Malyshev,
N. Bityurin, and A. Sergeev**

Institute of Applied Physics of Russian Academy of Sciences, Nizhny Novgorod, Uljanov st., 46,
Russia 603600

(Paper CDO-003 received Dec. 4, 1997; revised manuscript received Nov. 9, 1998; accepted for publication Nov. 13, 1998.)

ABSTRACT

We demonstrate that optical coherence tomography (OCT) is a convenient diagnostic tool to monitor pulse-to-pulse kinetics in laser interactions with biological tissue. In experiments on laser modification and ablation of the cataractous human lens and the porcine cornea we have applied this technique *in situ* to investigate different modes of preablation tissue swelling, crater formation and thermally affected zone development. The cataractous lens is an example of highly scattering media whereas the cornea is initially low scattering. The radiation with different wavelengths has been employed including that of a YAG:Er laser ($\lambda = 2.94 \mu\text{m}$), a glass:Er laser ($\lambda = 1.54 \mu\text{m}$), YAG:Nd lasers ($\lambda = 1.32 \mu\text{m}$ and $\lambda = 1.44 \mu\text{m}$), as well as of the fifth harmonic of a Nd:YAP laser ($\lambda = 0.216 \mu\text{m}$). Pulse-to-pulse OCT monitoring has been accompanied by the probe beam shielding diagnostics to provide the time-resolved observation of the interaction dynamics. © 1999 Society of Photo-Optical Instrumentation Engineers. [S1083-3668(99)00801-1]

Keywords optical coherence tomography; *in situ* monitoring; IR lasers; UV lasers; thermal tissue damage; pulse-to-pulse kinetics.

1 INTRODUCTION

Laser ablation of biological tissue involves many fascinating aspects of the fundamentals of laser interactions with composite materials.¹⁻⁴ From the practical point of view this process is of great importance for creation of a reliable laser scalpel. The radiation of IR and UV lasers is the most feasible candidate for that, because of the strong absorption by biological tissues. In the experiments reported here, several IR lasers with different wavelengths corresponding to different initial water absorption coefficients α are employed: a YAG:Er laser with the wavelength $\lambda = 2.94 \mu\text{m}$ ($\alpha \sim 10^4 \text{ cm}^{-1}$), a glass:Er laser with $\lambda = 1.54 \mu\text{m}$ ($\alpha \sim 10 \text{ cm}^{-1}$), and YAG:Nd lasers with $\lambda = 1.32 \mu\text{m}$ ($\alpha \sim 1 \text{ cm}^{-1}$) and $\lambda = 1.44 \mu\text{m}$ ($\alpha \sim 30 \text{ cm}^{-1}$). Strong variation in absorption by water has been expected to result in a significant difference in ablation and tissue modification kinetics. As a source of the UV laser radiation, the fifth harmonic of a Nd:YAP laser with the wavelength 216 nm is used.

The observation of biotissue modification processes by means of conventional optical techniques is difficult because of the high degree of light scattering by the tissue. The advent of a special technique for monitoring processes in turbid media, that is, optical coherence tomography (OCT), has allowed one to study laser-tissue interactions processes *in situ*. It enables one to control the ablation process as well as to monitor the laser-induced thermal damage in tissue layers adjacent to the ablation crater.⁵⁻⁸ The nondestructive observation of laser treated tissues permits elucidation of the hidden features in laser-matter interactions. This knowledge is of great importance for adequate modeling and optimization of laser surgery applications.

In the present paper, along with the ablation kinetics, we report the results of our experimental investigation on different kinds of biological material modifications, namely, creation of a dent and formation of a hump in a cataract-suffered lens due to the laser irradiation below the ablation threshold. An incubation was observed when the laser fluence was less than the threshold for a hump to appear after a single pulse. The hump is formed under the

L. Snopova is also at the Medical Academy, Nizhny Novgorod, Russia.

Address correspondence to V. Kamensky. Tel: +7 8312 384503; Fax: +7 8312 363792; E-mail: vlad@ufp.appl.sci-nnov.ru.

1083-3668/99/\$10.00 © 1999 SPIE

action of several pulses. The observation of the tissue surface with the temporal resolution of 2 ms, which is significantly smaller than the pulse train duration, reveals the evidence of the emergence of a nonstationary, "transient" hump.

2 MATERIALS AND EQUIPMENT

IR laser radiation was generated from a pulse YAG:Er laser (with wavelength $\lambda = 2.94 \mu\text{m}$ and pulse energy $E = 1 \text{ J}$), a YAG:Nd laser ($\lambda = 1.32, 1.44 \mu\text{m}$, $E = 800 \text{ mJ}$), and a glass:Er laser ($\lambda = 1.54 \mu\text{m}$, $E = 300 \text{ mJ}$). These lasers operate in the free-running regime with pulse train duration about $300 \mu\text{s}$. The radiation of all these lasers is mainly absorbed by water in biological tissues.

Among the used lasers the YAG:Er laser has the maximum value of absorption coefficient $\alpha \sim 10^4 \text{ cm}^{-1}$ and minimum thermally damaged layer. The YAG:Nd ($\lambda = 1.32 \mu\text{m}$) and glass:Er lasers are utilized since their wavelengths and, thus the depths of light penetration into the material, allow the observation of laser interaction with the material within the bulk of the highly scattering layer, which is difficult to perform with conventional diagnostic optical methods.

The fifth harmonic of a Q-switched YAP:Nd laser with the wavelength 216 nm, pulse energy up to 10 mJ, and the pulse-to-pulse energy stability within 4% was used as a source of UV laser radiation.⁹ These IR and UV lasers were specially constructed at the Institute of Applied Physics of Russian Academy of Sciences.

To monitor laser-tissue interaction, a compact self-made OCT device with a fiber optical interferometer flexible optical cable and an integrated piezoelectric in-depth scanning unit was used.⁷ The both in-depth and lateral spatial resolution of the OCT device is $15 \mu\text{m}$, the acquisition time for 200×200 pixels image is several seconds and the working wavelengths are 830 and 1260 nm. A diagnostic beam (collimated and focused from a fiber tip) was coupled with the high-power laser beam using a dichroic mirror allowing one the *in situ* observation of tissue modification.

Samples included the post-surgery human cataractous lens [nuclear 366.16 and total or subtotal 366.17 according to International Classification of Diseases, 9th Revision, Clinical Modification (ICD-9-CM)] and porcine cornea. The cornea was preserved during six hours, the lens could be kept up to two days in a normal saline solution. Since the biotissue surface is quickly drying in the air, measurements were limited to 20 min. While a healthy lens is optically transparent and quite homogeneous, a cataractous nuclear lens is optically opaque due to high scattering with different coefficients depending on the severity of the disease and cannot be observed with traditional optics. Immediately prior to use the epithelium covering the cornea was mechanically removed to expose the

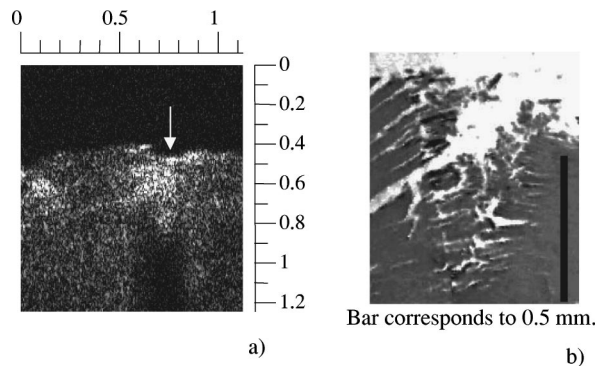


Fig. 1 (a) Comparison of a tomographical image with (b) a histological pattern. Cataracted lens irradiated by a YAG:Nd laser ($\lambda = 1.44 \mu\text{m}$).

stroma. A virgin porcine cornea is fairly low scattering, whereas the laser irradiation can result in a significant enhancement of scattering within the thermally affected zone.

A thermally damaged area is formed during laser modification. The last publications^{5,10} report an accordance of the thermally damaged area observed by OCT and by traditional histological study. This is also confirmed by our investigations of ablation of a cataractous lens at wavelength $1.44 \mu\text{m}$ (see Figure 1).

3 TISSUE MODIFICATIONS

First experimental data on OCT investigations of effects of laser radiation on retina in monkey eyes in Ref. 5. In this chapter we perform more comprehensive study of tissue swelling occurring due to laser irradiation below ablation threshold. This is illustrated in Figure 2 where tomograms of modification of a cataractous lens by glass:Er laser at different fluences are presented.

Radiation with fluence over $\sim 250\text{--}350 \text{ J/cm}^2$ causes ablation crater formation [Figure 2(a)]. At fluences close to threshold the material is swelling out and a hump is formed [Figure 2(b)]. At fluences below 100 J/cm^2 required for hump formation, a part of the surface is slowly desiccated and forms a dent [Figure 2(c)].

The kinetics of hump formation was studied in several sets of experiments. The first set was concerned with the single shot response of tissue. Each laser pulse irradiated only a virgin area of the material. The fluence was increased from pulse to pulse. Figure 2(b) shows the formation of a hump with the height up to 0.2 mm over the irradiated surface. For a given sample, the hump formation occurs within a small interval of fluences. The increase in the laser fluence above threshold value up to 200 J/cm^2 does not result in a visible increase of the hump height but rather in some increase in its width.

The second set of experiments was related to incubation effects. Irradiation of the same part of the

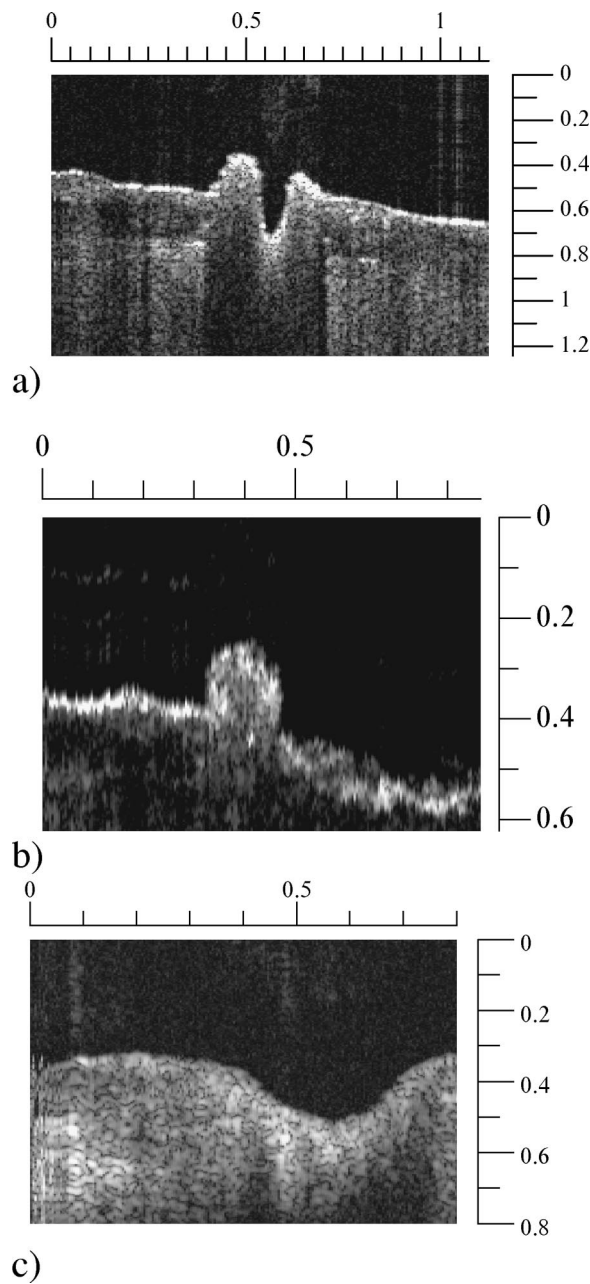


Fig. 2 Tomograms of a cataractous lens modification due to irradiation by a glass:Er laser at different fluences: (a) laser fluence 40 J/cm^2 after 10 pulses with repetition rate $f=0.05 \text{ Hz}$, (b) laser fluence 250 J/cm^2 after 1 pulse, (c) laser fluence 400 J/cm^2 after 1 pulse.

tissue was performed by several laser pulses with fluences less than the threshold value. The repetition rate was one pulse per 25 s which was slow enough to avoid the heat accumulation in the treated zone from pulse to pulse.

The result is demonstrated in Figure 3. It is seen that the effect of successive subthreshold pulses manifests itself by the creation and development of a cloudy zone beneath the surface with subsequent formation of a hump. It is worth noting that the height of the developed hump decreases and the

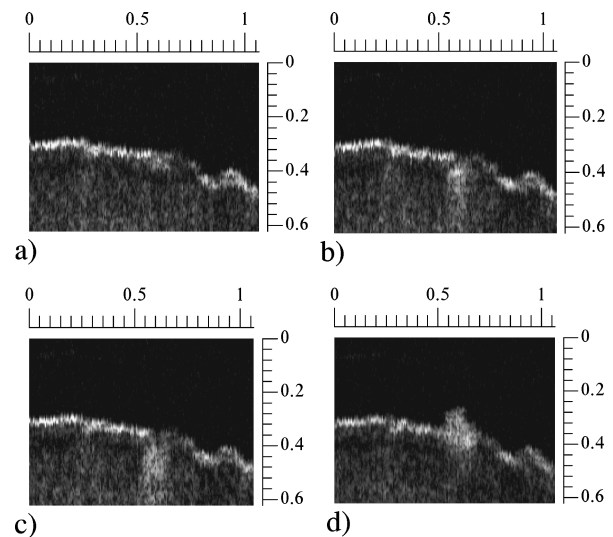


Fig. 3 Pulse-to-pulse kinetics of hump growth (glass:Er; $\lambda = 1.54 \mu\text{m}$). Fluence is 60% of the threshold value. (a) no pulse, (b) 1 pulse, (c) 3 pulses, (d) 4 pulses. Scale unit corresponds to 1 mm.

amount of pulses needed to create the hump increases with the decrease in the fluence. The simple estimations allow us to suppose that transformations accounted for the hump formation are connected with heating of the material up to 100°C and probably with partial vaporization of water.

In this study cataractous lenses are utilized with a different water mass content ($\pm 5\%$) and therefore somewhat different initial optical and mechanical properties. This may account for the scattering in data on the threshold fluence from sample to sample.

The hump growth may be attributed to nonelastic viscous flow driven by the pressure of water heated due to the laser irradiation and evaporating at temperatures somewhat higher than 100°C . The incubation may be connected with the gradual changing in mechanical and thermophysical properties of subsurface layers of the irradiated material resulting from the partial dehydration of tissue and collagen denaturation. These changes cause the decrease of thermal diffusivity due to creation of pores and the loss of elasticity due to modification of the material.

To observe the laser modification dynamics with the temporal resolution, which is comparable to the pulse train duration, the changes in transmission of the probe radiation from the single transverse mode (TEM_{00}) stabilized cw $0.83 \mu\text{m}$ diode laser are measured. The cw laser radiation is transported perpendicular to the beam of the high-power glass:Er laser and close to the tissue surface. The oscillograms (see Figure 4) show the effect of blocking of a cw beam by a cataractous lens material, which is swelled out due to interaction of the high-power radiation with the lens. When the laser fluence was smaller than the threshold, the emergence of a "transient hump" which disappears after sev-

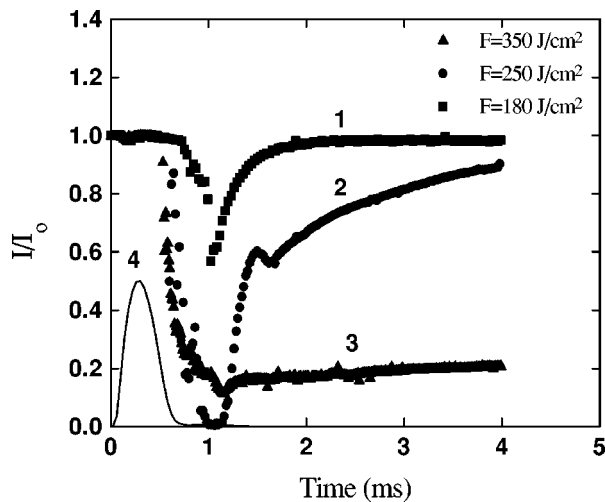


Fig. 4 Oscillograms of shielding of cw laser probe radiation by hump. I_0 , initial intensity of probe cw laser. Free-running glass:Er laser irradiation of cataractous lens. F —fluence. 1,2—transient hump, 3—stationary hump creation, 4—pulse shape (arbitrary units).

eral milliseconds was observed. (See curves 1 and 2, Figure 4.) When the fluence is higher than the threshold value, the probe radiation is blocked off according to the oscillogram 3 (Figure 4). After irradiation the remaining hump can be visually observed. To prove that this effect does not occur as a response of the whole object to the blowing up of decomposition products, the transmittance of the probe radiation 1 mm aside from the treated zone along the lens surface was studied. The probe radiation is not blocked in this case.

The swelling of cornea due to heating is well known and widely used in photothermal keratoplasty treatment,¹¹ where YAG:Ho laser radiation is commonly employed. This effect is usually associated with denaturation of collagens.¹¹ The above experimental data on formation of a hump on the cataractous lens under the effect of a glass:Er laser allow us to suggest that thermal denaturation of proteins may not be solely involved in this process. The temporal swelling, or “transient hump,” does not correlate with the irreversible thermal denaturation. Mechanical stresses are implicated here and the irreversible hump may be attributed to the non-elastic viscous flow driven by the pressure of water heated by laser irradiation and evaporating at temperatures somewhat higher than 100 °C.

It should be noted that hump formation due to irradiation of the surface of artificial polymers below the ablation threshold has been studied, e.g., in papers from Refs. 12 and 13. The nature of preablation swelling is still controversial. In the above considered case of irradiation of the cataractous lens by a glass:Er laser, hump formation is much more pronounced and can be studied in more detail. We believe that this facilitates establishing the similarity

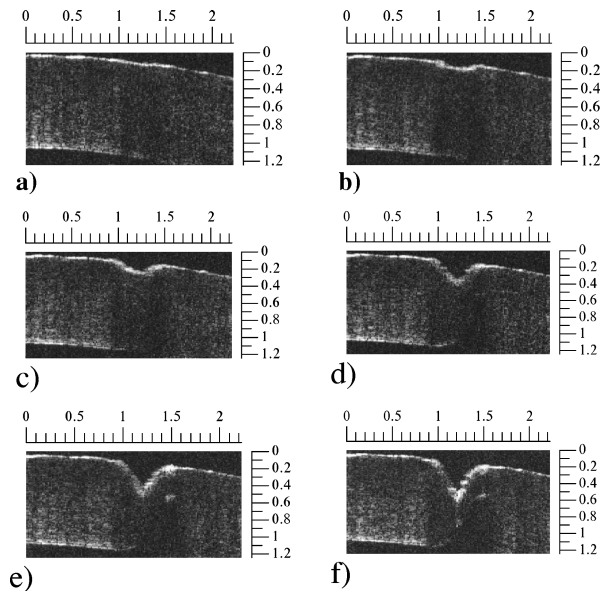


Fig. 5 Kinetics of pulse-to-pulse layer-by-layer crater growth due to irradiation by YAG:Er laser (repetition rate 3 Hz, pulse train energy – 15 mJ), (a) initial, (b) 20 s, (c) 50 s, (d) 100 s, (e) 150 s, (f) 200 s. Scale unit corresponds to 1 mm.

between the resembling phenomena in different materials.

4 ABLATION REGIMES

In experiments at higher fluences OCT clearly records the pulse-to-pulse kinetics of the ablation crater growth. Figure 5 represents the pulse-to-pulse kinetics of the crater growth due to YAG:Er laser irradiation of tissue. Because of the high value of absorption coefficient ($\sim 10^4 \text{ cm}^{-1}$) the formation of the crater is a step-by-step process. Using the OCT technique can, in principle, follow not only the depth of crater but also the rise and development of a thermally damaged layer adjacent to the crater surfaces.^{14–16} As it can be seen in Figure 5, in the case of ablation of a lens by the YAG:Er laser, the thickness of the thermally damaged layer is comparable with the OCT resolution limit, which is 15 μm .

A different ablation kinetics is observed when using a YAG:Nd laser with the wavelength of 1.32 μm . The corresponding absorption coefficient is about 1 cm^{-1} . In this experiment, the repetition rate was 20 Hz, the pulse energy was 40 mJ, the laser beam was focused onto the surface of the lens in a spot with the diameter of 80 μm , the Rayleigh length was estimated to be about 2 mm. The evolution of tissue during irradiation, lasting for approximately 12 min, is shown in Figure 6. It can be seen that the laser heating causes the essential tissue modification which manifests itself in a scattering enhancement [compare Figures 6(a) and 6(b)], cavern formation [Figures 6(c) and 6(d)], and an essential swelling of the lens surface [Figures 6(d) and

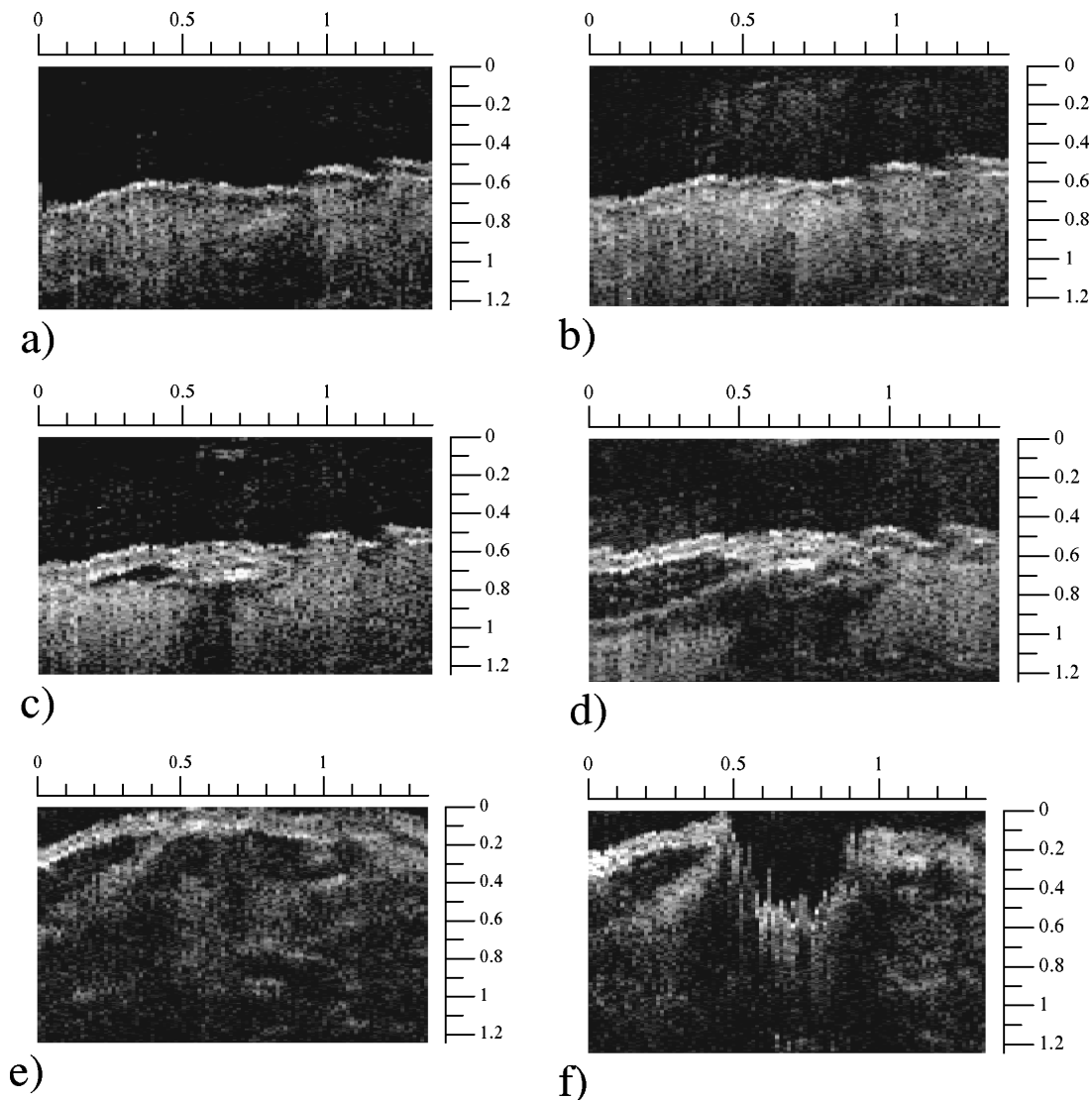


Fig. 6 Effect of heat accumulation. Modification and swelling followed by blow up elimination of material. (YAG:Nd, $\lambda = 1.32 \mu\text{m}$, repetition rate 20 Hz, pulse energy 40 mJ, laser spot diameter $80 \mu\text{m}$.) Scale unit corresponds to 1 mm.

6(e)]. The incremental swelling is followed by an abrupt blow up process of crater creation (Figure 6). The pictured crater has been created for a few pulses after more than 12 min of irradiation at a rate of 20 pulses per second.

Irradiation of the lens results in substantial integrated heating not only of the irradiated area but also of the great part of adjacent material. The simple estimations of absorbed energy are in general agreement with the assumption that the reason for crater formation is the pressure induced by evaporated water with the temperature somewhat higher than 100°C . This overheating may be caused by the resistance to water elimination rendered by the dried and strongly modified outer part of the tissue. It should be noted, however, that the mechanism of the described explosion has not yet been completely understood. As can be deduced from tomograms in Figure 6, the drying of

the irradiated area may result in essential changing of properties of modified material including a decrease in thermal diffusivity. The latter may cause the heating confinement. Thus, the temperature involved may appear to be essentially higher than 100°C . The surface of the crater walls was covered by the black residue which could be related to products of protein pyrolysis.

Figure 7 exhibits the hump transformations during multishot irradiation by the glass:Er laser with the wavelength of $1.54 \mu\text{m}$ in free-running mode with a fluence somewhat higher than the ablation threshold. The corresponding absorption coefficient of water is 12 cm^{-1} . The spot diameter was $200 \mu\text{m}$. The laser beam was focused onto the surface of the material. It can be seen that in this case the hump growth is followed by the ablation crater digging inside the swollen zone.

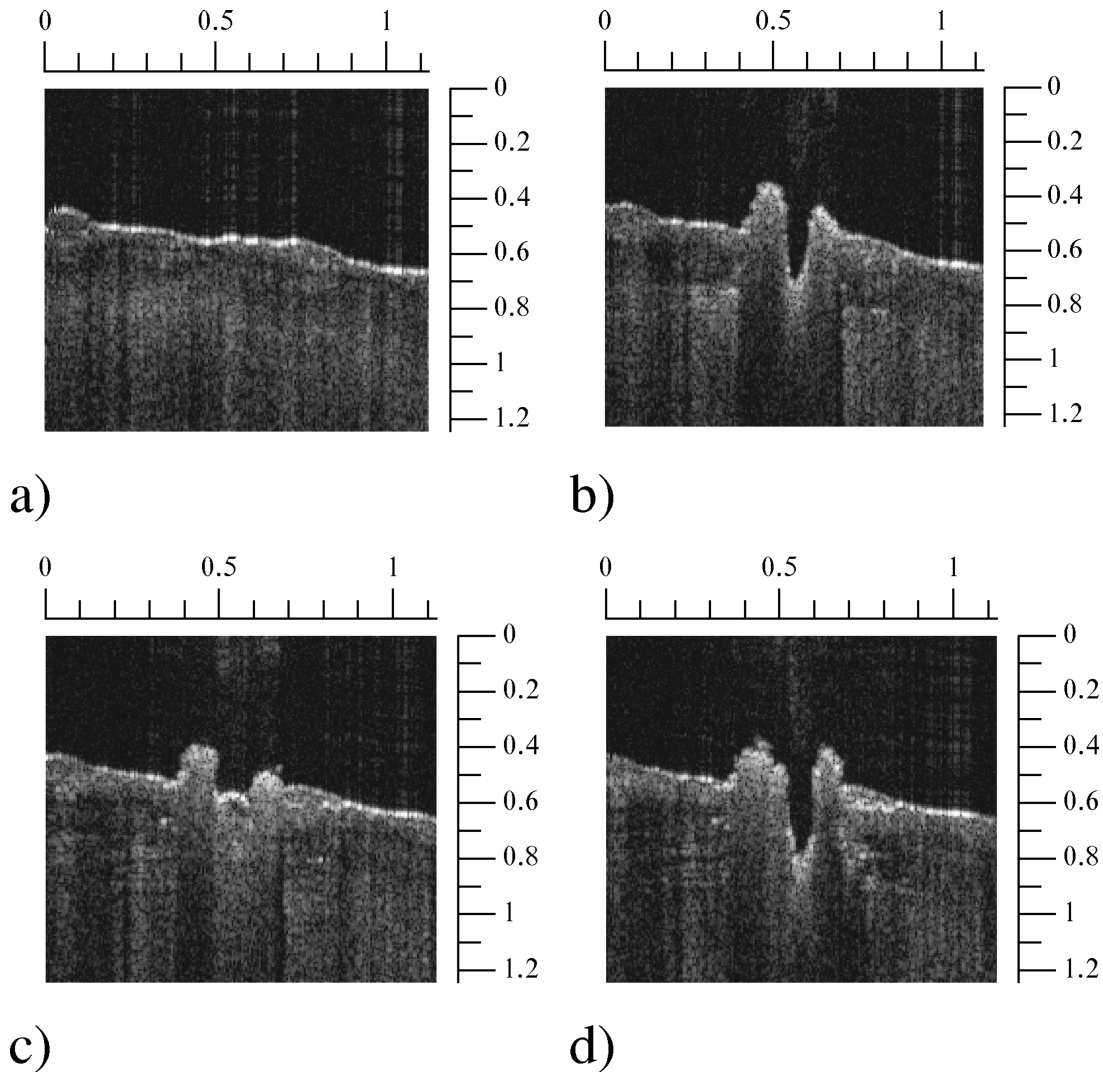


Fig. 7 Pulse-to-pulse kinetics. "Self-oscillatory" ablation-hump formation. The beam was tightly focused on the surface (glass:Er; $\lambda = 1.54 \mu\text{m}$). (a) Initial, (b) 10 pulses, (c) 22 pulses, (d) 30 pulses. Scale unit corresponds to 1 mm.

It is interesting to note that the ablation process itself may have a complex kinetics when the formation of an ablative crater is changed by a hump growing and vice versa. A "self-oscillatory" pulse-to-pulse kinetics during irradiation of a lens by a tightly focused beam was observed. The focus was located at the very surface of the sample. This regime is illustrated in Figure 7.

Figure 8 exhibits the pulse-to-pulse kinetics of ablation crater growth in the porcine cornea during UV irradiation. The UV radiation is absorbed by protein chromophores. The thermally damaged zone is not seen here. This is in agreement with the histological investigation of the superficial layer of the ablated crater formed during irradiation by an ArF excimer laser.¹⁷ It should be mentioned, however, that the absorption coefficient of collagen at wavelength 193 nm is higher than that at the wavelength of the fifth harmonic.¹⁸ The latter is close to the value of the absorption coefficient at the wave-

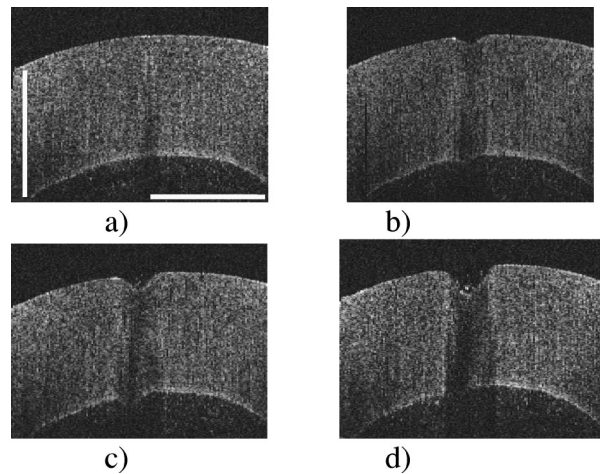


Fig. 8 Kinetics of ablation crater growth under the effect of YAP:Nd laser fifth harmonic radiation (repetition rate was 10 Hz, pulse energy was 0.7 mJ). (a) Initial, (b) after 10 s, (c) 30 s, (d) 70 s. Bar corresponds to 1 mm.

length of a YAG:Er laser. This fact stimulated us to study the combined effect of IR and UV radiation on cornea,¹⁹ which will be addressed in detail in our forthcoming publication.

5 CONCLUSION

OCT is a convenient technique to follow the pulse-to-pulse transformation kinetics of superficial layers of turbid biological tissues under the action of the laser radiation. This was proved by monitoring of the response of the cataractous human lens and the porcine cornea to irradiation by several mid-infrared and UV lasers.

The features of hump formation on the surface of the cataractous human lens under the action of mid-IR laser radiation were studied in detail. These observations allow us to propose that hump creation can be attributed to elastic ("transient" hump) or nonelastic viscous flow of the material driven by the pressure induced by heated and partly evaporated water.

Besides layer-by-layer ablation by the highly absorbed radiation YAG:Er laser with wavelength $\lambda = 2.94 \mu\text{m}$ and the fifth harmonic of a Nd:YAP laser ($\lambda = 216 \text{ nm}$) we follow also ablation with incubation at slow absorption (a YAG:Nd lasers with $\lambda = 1.32 \mu\text{m}$) and ablation accompanied by hump formation for the intermediate case (a glass:Er laser with $\lambda = 1.54 \mu\text{m}$).

The OCT technique is suitable to estimate *in situ* the size of the thermally damaged layer adjacent to the ablation crater created due to laser irradiation at different wavelengths with different initial values of the absorption coefficient of water.

The advantage of OCT monitoring in these investigations is the capability to follow the transformations of layers that are hidden for usual optical observation. The behavior of these layers precedes the subsequent events on the surface of irradiated tissue.

Acknowledgments

This work has been supported in part by the Russian Foundation for Basic Researches. The authors are grateful to the staff of Nizhny Novgorod City Hospital No. 35 and in particularly to Dr. N. V. Artemiev for the assistance in this study.

REFERENCES

1. A. J. Welsh, M. Motamedi, S. Rastegar, G. L. LeCarpentier, and E. D. Jansen, "Laser thermal ablation," *Photochem. Photobiol.* **53**, 815–823 (1991).
2. S. L. Jacques, "Laser-tissue interactions: photochemical, photothermal and photomechanical," *Surg. Clin. North Am.* **72**, 531–558 (1992).
3. B. Ross and C. Puliafito, "Erbium-YAG and Holmium-YAG laser ablation of the lens," *Lasers Surg. Med.* **1**, 74–82 (1994).
4. G. Edwards, R. Logan, M. Copeland, L. Reinisch, J. Davidson, B. Johnson, R. Maclunas, J. Mendenhaven, R. Ossoff, J. Tribble, J. Werkhaven, and D. O'Day, "Tissue ablation by a free-electron laser tuned to the amide II band," *Nature (London)* **371**, 416–419 (1994).

5. R. Birngruber, M. R. Hee, S. A. Boppart, J. G. Fujimoto, E. A. Swanson, C. A. Toth, C. D. Di Carlo, C. P. Cain, G. D. Noojin, and W. P. Roach, "In vivo imaging of the development of linear and non-linear retinal laser effects using Optical Coherence Tomography in correlation with histopathological findings," in *Laser-Tissue Interaction, BIOS'95*, S. L. Jacques, Ed., *Proc. SPIE* **2391**, 21–27 (1995).
6. V. Kamensky, V. Gelikonov, G. Gelikonov, K. Pravdenko, N. Bityurin, A. Sergeev, F. Feldchtein, A. Pushkin, I. Skripachev, and M. Tshurbanov, "YAG:Er laser system for eye microsurgery with OCT monitoring," *CLEO, OSA Tech. Dig. Ser.* **9**, 60 (1996).
7. A. M. Sergeev, V. M. Gelikonov, G. V. Gelikonov, F. I. Feldchtein, N. D. Gladkova, and V. A. Kamensky, "Biomedical diagnostics using optical coherence tomography," *OS TOPS* **2**, 196 (1996); G. V. Gelikonov, V. M. Gelikonov, F. I. Feldchtein, J. P. Stepanov, A. M. Sergeev, I. Antoniou, J. Ioannovich, D. H. Reitze, and W. W. Dawson, "Two-color-in-one-interferometer OCT system for bioimaging," *CLEO, OSA Tech. Dig. Ser.* **11**, 210 (1997).
8. C. A. Toth, R. Birngruber, S. A. Boppart, M. R. Hee, J. G. Fujimoto, C. D. Di Carlo, S. A. Swanson, C. P. Cain, D. G. Narayan, G. D. Noojin, and W. P. Roach, "Argon laser retinal lesions evaluated *in vivo* by optical coherence tomography," *Am. J. Ophthalmol.* **123**(2), 188–198 (1997).
9. S. V. Muraviov, A. A. Babin, F. I. Feldchtein, A. M. Yurkin, V. A. Kamensky, A. Yu. Malyshev, M. S. Kitai, and N. M. Bityurin, "Efficient conversion to the fifth harmonic of spatially multimode radiation of a repetitively pulsed Nd:YAP laser," *Quantum Electron.* **28**(6), 520–521 (1998).
10. N. Koop, R. Brinkmann, B. Kaftan, M. Asiyovogel, R. Engelhardt, and R. Birngruber, "Comparison of thermal corneal lesions by OCT and polarization histology," in *Lasers in Ophthalmology IV*, R. Birngruber, A. F. Fercher, and Ph. Sourdille, Eds., *Proc. SPIE* **2930**, 216–221 (1996).
11. Q. Ren, R. H. Keates, R. A. Hill, and M. W. Berns, "Laser refractive surgery: a review and current status," *Opt. Eng.* **34**(3), 642–659 (1995).
12. M. Himmelbauer, E. Arenholz, D. Bäuerle, and K. Schilcher, "UV-laser-induced surface topology changes in polyimide," *Appl. Phys. A: Solids Surf.* **63**, 337–339 (1996).
13. M. Himmelbauer, N. Arnold, N. Bityurin, E. Arenholz, and D. Bäuerle, "UV-laser-induced periodic surface structures on polyimide," *Appl. Phys. A: Solids Surf.* **64**, 451–455 (1997).
14. V. Kamensky, V. Gelikonov, G. Gelikonov, F. Feldchtein, A. Sergeev, K. Pravdenko, N. Artemiev, N. Bityurin, I. Skripachev, A. Pushkin, and G. Snopatin, "In situ monitoring of the mid-IR laser ablation of cataract-suffered human lens by optical coherent tomography," in *Lasers in Ophthalmology IV*, R. Birngruber, A. Fercher, and P. Sourdille, Eds., *Proc. SPIE* **2930**, 222–229 (1996).
15. F. Feldchtein, V. Kamensky, K. Pravdenko, V. Gelikonov, G. Gelikonov, A. Sergeev, and N. Bityurin, "Monitoring and animation of laser ablation process in cataracted eye lens using coherence tomography," in *Coherence Domain Optical Methods in Biomedical Science and Clinical Applications*, V. Tuchin, H. Podbielska, and B. Ovrzyn, Eds., *Proc. SPIE* **2981**, 94–102 (1997).
16. V. Kamensky, R. Kuranov, G. Gelikonov, S. Muraviov, A. Malyshev, A. Yurkin, F. Feldchtein, and N. Bityurin, "In situ observation of IR and UV solid state laser modifications of lens and cornea," in *Laser-Tissue Interaction IX*, S. L. Jacques, Ed., *Proc. SPIE* **3254**, 390–397 (1998).
17. M. N. Asiyovogel, R. Brinkmann, H. Notbohm, R. Eggers, H. Lubatschowski, and H. Laqua, and A. Vogel, "Histologic analysis of thermal effects in laser thermokeratoplasty and corneal ablation using sirius-red polarization microscopy," *J. Cataract Refractive Surg.* **23**(4), 515–526 (1997).
18. M. N. Ediger, G. H. Pettit, and D. W. Hahn, "Enhanced ArF laser absorption in a collagen target under ablative conditions," *Lasers Surg. Med.* **15**, 107–111 (1994).
19. N. M. Bityurin, V. A. Kamensky, S. V. Muraviov, F. I. Feldchtein, A. Yu. Malyshev, A. M. Sergeev, L. B. Snopova, and A. M. Yurkin, "Combined effect of IR and UV laser radiation on biological tissues: cleaning," *CLEO, OSA Tech. Dig. Ser.* **6**, 230 (1998).